Supplemental Data

Methods for Supplemental Figures

Mice

pOBCol2.3GFPemd (COL2.3GFP) mice (now available at Jackson Laboratories, Bar Harbor, Maine), in which GFP expression is limited to mature osteoblasts through the collagen 2.3kb promoter, were originally generously provided by Dr. Hyun-Duck Nah (The Children's Hospital of Philadelphia, Philadelphia, PA).

Histology

Immunostaining of paraffin-embedded sections was performed using rabbit anti-GFP antibody (Invitrogen; Carlsbad, CA), goat anti-rabbit biotinylated secondary antibody (1:180), avidin/biotin complexes and NovaRED peroxidase development (Vector Laboratories). Immunofluorescent staining was performed on 6 µm thickness paraffin embedded sections. After blocking with 10% donkey serum, sections were stained with goat anti-GFP polyclonal antibody (1:200, Novus Biologicals) and rabbit anti-PDGFRβ polyclonal antibody (1:150, Santa Cruz Biotechnology) at 4˚C overnight. Sections were subsequently stained with secondary antibodies (Alexa Fluor 488 donkey anti-goat antibody and alexa 555 donkey anti-rabbit antibody, 1:250, Life Technologies) for 1.5 hours at room temperature, and then with 4',6-diamidino-2-phenylindole (DAPI, Life Technologies). Pictures were acquired with a digital AxioCam HRc camera attached to a Zeiss AxioImager.A1 using 20x/0.5NA dry or 40x/0.75 NA dry-objective lenses and AxioVision 4.5 software (Carl Zeiss MicroImaging LLC).

Real-time rt-PCR

To obtain endosteal osteoblasts for Real-time rt-PCR, bone marrow cells were removed by flushing femur and tibia of COL2.3GFP mice, empty bones were dissected into small fragments

and digested for 3 hours at 37°C with collagenase P (0.2 mg/mL; Roche Diagnostics) in Dulbecco's modified Eagle medium-Ham's F12 mixture supplemented with 2 mM L -glutamine, 100 U/mL penicillin/streptomycin (Mediatech Inc.). Cells were collected by centrifuging at 300g for 5 min, and sorted using the BD FACSAria (BD Biosciences) to isolate the $CD45^-$ GFP^+osteoblast fraction. $CD45^+GFP^-$ cells from BM were also isolated as a comparison population. RNAs were isolated from the sorted cells with either the RNeasy micro kit (Qiagen) or Trizol Reagent (Life Technologies) according to manufacturer instructions. As an additional control population, peripheral blood mononuclear cells were collected from the retro-orbital sinus of WT mice and RNA was collected with Trizol LS Reagent (Life Technologies). cDNAs were synthesized with High Capacity cDNA Reverse Transcription Kit (Life Technologies). Quantitative PCR was performed with Taqman Gene Expression Assays for PDGFRβ and GAPDH using Applied Biosystems 7500 Fast Real-Time PCR Systems (Life Technologies) according to manufacturer instructions, and the data were analyzed with 7500 software v2.0 (Life Technologies).

Sca-1$^+$ Donor BM Primary Transplant Assay

GFP^+ donor BM was harvested from femur/tibia of H2K-GFP donor mice. BM was incubated with PE-labeled anti-SCA-1 antibody (LY-6A/E) (BD Biosciences) at 4^0 for 20 minutes, followed by incubation with Anti-PE microbeads (Miltenyi Biotec). Cells were then magnetically selected on the basis of SCA-1 expression using the Miltenyi AutoMACS system according to manufacturer's protocol. After confirmation of selection of SCA-1^+ cells by flow cytometry, SCA-1^+ BM cells were transplanted by tail vein injection at a dose of 1.75×10^6 cells/mouse into primary recipient WT, anti-CD41 treated WT, and *mpl*$^{-/-}$ mice 48 hours post-TBI. 36 hours after transplant, all bone marrow from bilateral femora/tibae from primary recipient mice was harvested and analyzed by flow cytometry for GFP, lineage (lin), c-Kit, and SCA-1 expression as described in the main Materials and Methods section.

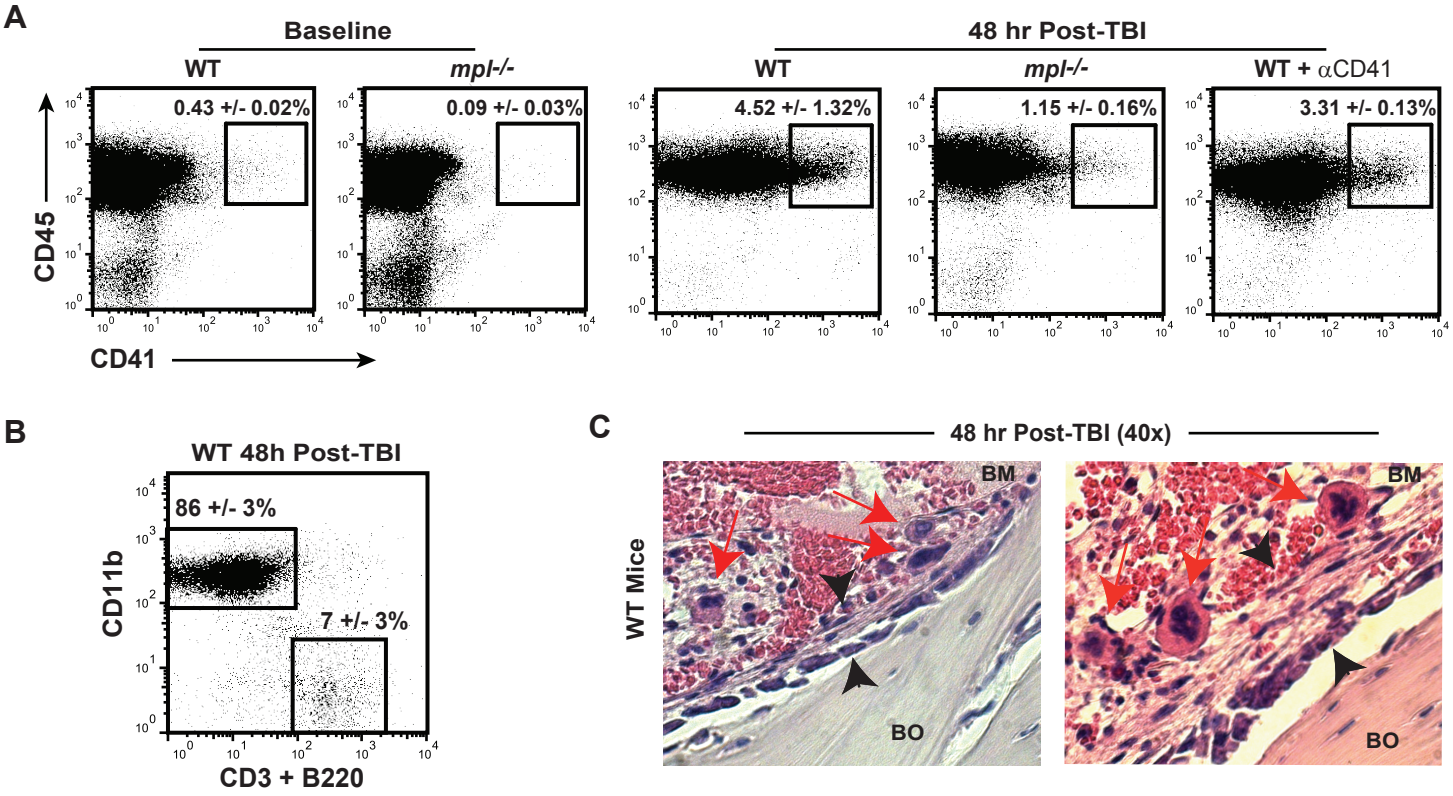

Supplemental Figure S1

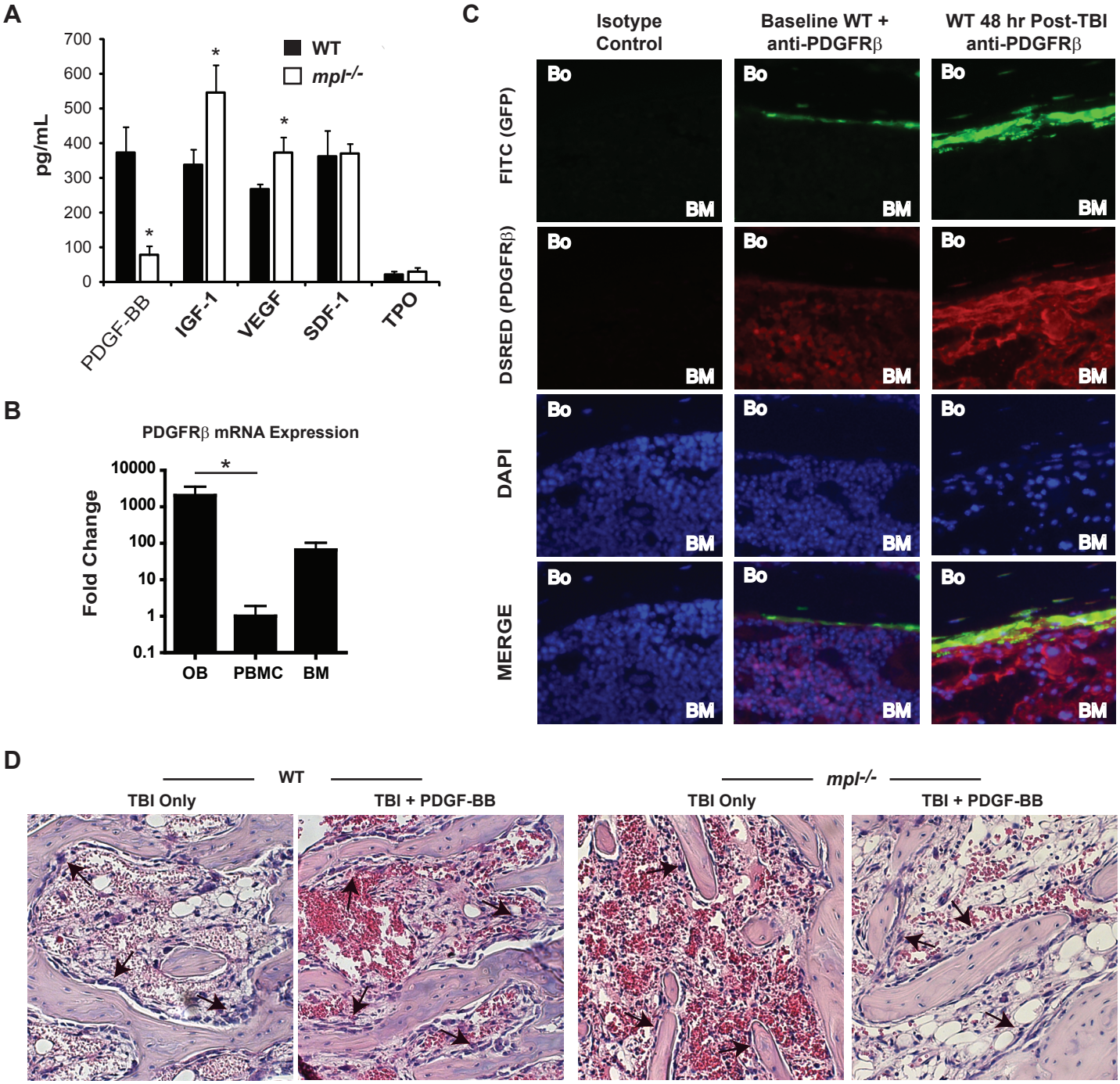

Supplemental Figure S2

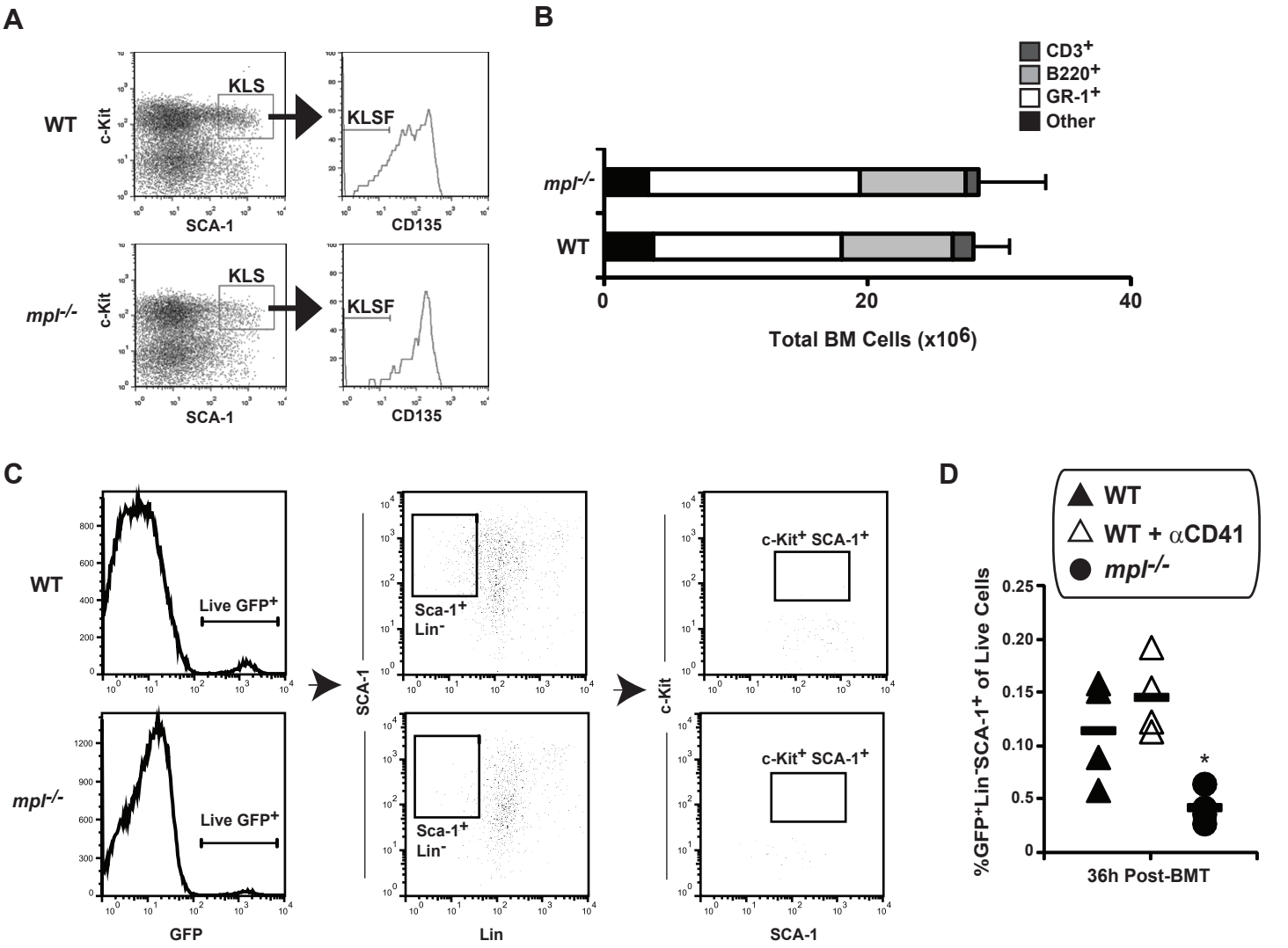

Supplemental Figure S3

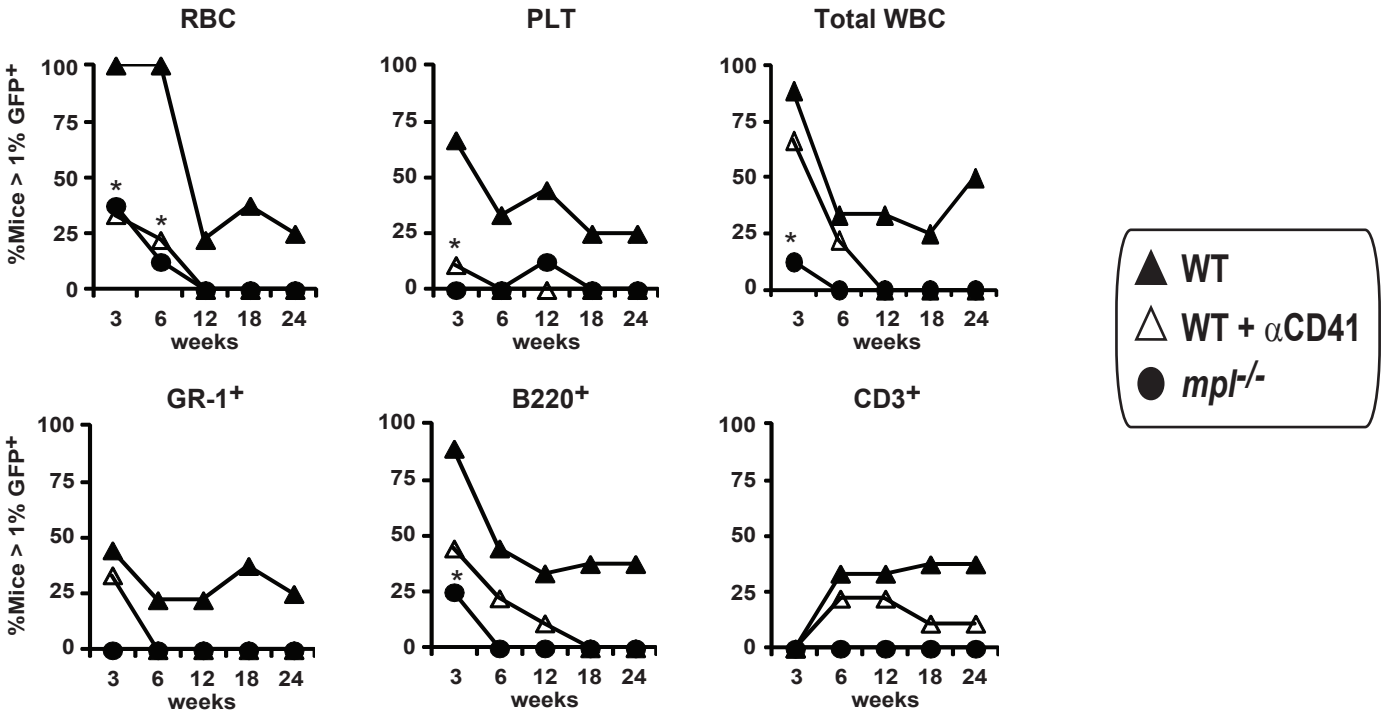

Supplemental Figure S4

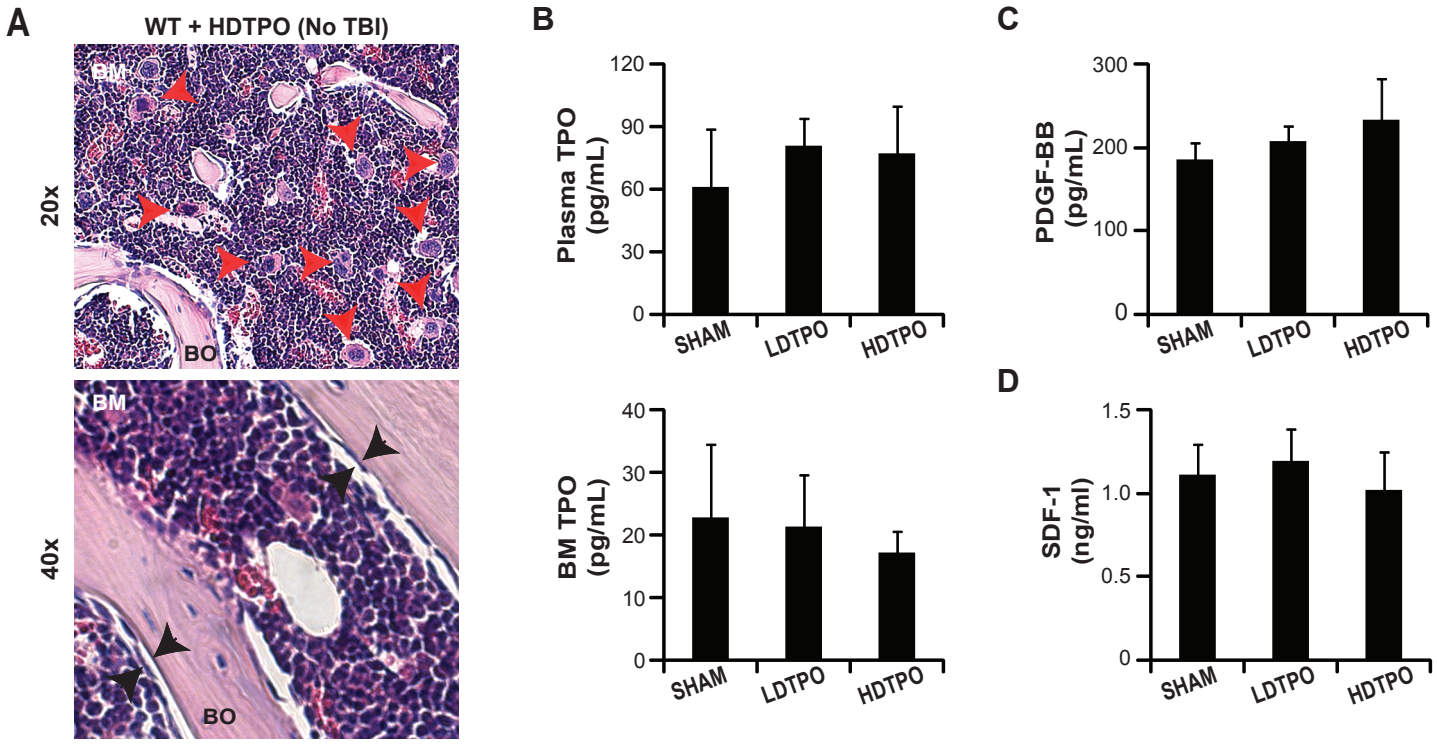

Supplemental Figure S5

Supplemental Figure Legends

Supplemental Figure S1: Examination of Pre- and Post-TBI bone marrow megakaryocyte populations and endosteal osteoblast expansion (related to Figures 1 and 2). (A) Flow cytometry dotplots gated on live cells, showing the percentage (mean ± SD) of all live bone marrow (BM) cells that are megakaryocytes ($CD45^+CD41^+$) at baseline (left 2 panels) and 48 hours post-TBI (right 3 panels) in WT mice (n=3 each), *mpl*$^{-/-}$ mice (n=3 each) and anti-CD41 treated WT mice (n=2). Data demonstrate that selective survival of megakaryocytes post-TBI results in increased relative percentages of megakaryocytes in BM post-TBI versus baseline, and that c-MPL deficiency, but not anti-CD41 treatment, results in decreased total megakaryocytes both at baseline and at 48 hours post-TBI. (B) Flow cytometry dotplot of WT bone marrow (gated on all live cells) 48 hours post-TBI, demonstrating that the majority of residual cells in BM at 48 hours post-TBI are myeloid ($CD11b^+$) and not lymphoid ($CD3^+/B220^+$). (C) H+E sections (40x) of metaphyseal bone (BO) and bone marrow (BM) from WT mice 48 hours post-TBI demonstrating that megakaryocytes (red arrows) preferentially migrate to the endosteum following TBI specifically to sites of endosteal osteoblast expansion (black arrowheads). (D) Immunostaining for GFP expression (red-brown) in bone marrow sections (40x) at baseline (left) and 48 hours post-TBI (right) from COL2.3GFP mice, in which GFP is selectively expressed by mature osteoblasts/osteocytes, demonstrating that TBI-induced endosteal expansion is primarily comprised of expanding mature osteoblasts.

Supplemental Figure S2: PDGF-BB and PDGFRβ play critical roles in TBI-induced endosteal osteoblast expansion (related to Figure 3). (A) Comparison of bone marrow (BM) levels of PDGF-BB, IGF-1, VEGF, SDF-1, and TPO by ELISA (mean ± SD) at baseline in WT versus *mpl*$^{-/-}$ mice (n= 5 mice each). At baseline, *mpl*$^{-/-}$ BM has only 21% of the PDGF-BB expression seen in WT BM, but increased IGF-1 and VEGF expression. *$p < 0.001$ by t-test for

comparison of *mpl*$^{-/-}$ versus WT expression. (B) mRNA expression of PDGFRβ by real-time rt-PCR (normalized to GAPDH expression) from isolated bone marrow osteoblasts (OB), peripheral blood mononuclear cells (PBMC), and whole BM cells (n = 3 each), demonstrating that endosteal osteoblasts have the highest levels of PDGFRβ expression among these populations. *Significantly increased ($p < 0.05$ by Kruskal-Wallis multiple comparison test for non-parametric data) expression in OB versus PBMC. (C) Immunofluorescent staining for GFP (green) and PDGFRβ (red) compared to isotype control, (co-stained for nucleated cells with DAPI, blue) on paraffin embedded metaphyseal bone (BO) and BM sections (40x magnification) at baseline or 48 hours post-TBI from COL2.3GFP mice, in which GFP is expressed specifically by endosteal osteoblasts. Images demonstrate that while PDGFRβ is expressed by a number of cells throughout BM, its expression is particularly high in the expanded endosteal osteoblast population post-TBI that, in this transgenic model, co-expresses GFP (MERGE pictures, bottom row). (D) Low power (20x) photomicrographs of H+E stained metaphyseal bone marrow sections at 48 hours post-TBI in WT and *mpl*$^{-/-}$ mice that received either TBI only or TBI + PDGF-BB (0.5 mg/kg/dose I.V.) every 12 hours post-TBI. Images demonstrate increased endosteal osteoblast proliferation (black arrows) in both WT and *mpl*$^{-/-}$ BM when treated with PDGF-BB post-TBI versus animals receiving TBI alone.

Supplemental Figure S3: Baseline and post-transplant comparisons of HSC/progenitor cell populations in WT versus *mpl*$^{-/-}$ mice (Related to Figure 4). (A) Representative flow cytometry dotplots and histograms showing gating strategy for determination of long term (LT)-HSC in WT and *mpl*$^{-/-}$ BM at baseline, defined by the CD135^{lo} (KLSF) subpopulation of Lin^{-}SCA-1^{+}c-kit^{+} (KLS) cells. (B) Average absolute baseline BM cellularity from 1 leg (femur + tibia) in WT and *mpl*$^{-/-}$ mice, subdivided into GR-1^{+} myeloid, B220^{+} B cell, CD3^{+} T cell and remaining cell (Other) populations (n=3 each), based on flow cytometry-determined subpopulation percentages. (C) Representative flow cytometry analysis from a primary transplant experiment in which WT, *mpl*$^{-/-}$, or anti-CD41 treated WT recipients (n = 4 each) received 1.75 x 10^{6} sorted

SCA-1$^+$GFP$^+$ donor BM cells, and at 36 hours post-transplant, all bone marrow from bilateral femora and tibae was assessed by flow cytometry to determine presence of cells with a KLS phenotype. Plots show the fraction of GFP$^+$ cells within all live cells (left), the fraction of lin$^-$Sca-1$^+$ cells within all live GFP$^+$ cells (middle), and the lack of cells with c-Kit$^+$ surface phenotype within the lin$^-$Sca-1$^+$ fraction (right) from both WT (top) and *mpl*$^{-/-}$ mice. (D) Quantitative analysis of the number of GFP$^+$Lin$^-$SCA-1$^+$ cells, expressed as a percentage of all live cells, in WT, *mpl*$^{-/-}$, or anti-CD41 treated WT recipients 36 hours after the Sca-1$^+$GFP$^+$ donor cell BMT described in (C). *Significantly decreased GFP$^+$Lin$^-$SCA-1$^+$ cells in *mpl*$^{-/-}$ recipients compared to WT or anti-CD41 treated WT recipients ($p < 0.05$ by one way ANOVA).

Supplemental Figure S4: Competitive secondary transplant performed 24 hours after primary transplant results in mostly short term engraftment of primary recipient BM (Related to Figure 5). Long-term follow-up of competitively transplanted WT secondary (2°) recipients receiving unirradiated WT competitor BM (2 x 10^5 cells), along with BM harvested from WT, WT + αCD41, or *mpl*$^{-/-}$ primary (1°) recipients (5% BM equivalent dose, meaning 1/5th of all harvested marrow from bilateral femora and tibiae in one primary recipient) 24 hours after 1^0 recipient BMT with GFP$^+$ BM (5 x 10^6 cells). Data show the fraction of 2° recipients of WT, WT + αCD41, or *mpl*$^{-/-}$ 1° recipient cells that demonstrate >1% GFP$^+$ cells from 3 to 24 weeks post-2° transplant within the peripheral red blood cell (RBC), platelet (PLT), total white blood cell (WBC, gated by forward and side scatter),myeloid (GR-1$^+$), B cell (B220$^+$), and T cell (CD3$^+$) lineages. *Significantly decreased percentage of mice with GFP$^+$ cells in specified lineage in 2° recipients of WT + αCD41 or *mpl*$^{-/-}$ versus WT 1° recipient cells ($p < 0.05$ by Fisher's Exact Test/contingency table analysis). The majority of 2° recipients of WT 1^0 recipient BM have GFP$^+$ reconstitution in all lineages but CD3$^+$ T cells in the first few weeks post 2° BMT, but most become GFP$^-$ (< 1% GFP$^+$ cells) in all lineages at later time points, demonstrating that much of the high initial GFP$^+$ engraftment post-2° BMT, when 2° BMT is performed 24 hours post-1° BMT, is due to ST-HSC and progenitors, and not to GFP$^+$ LT-HSC engraftment.

Supplemental Figure S5: Effect of Thrombopoietin (TPO) administration on endosteal osteoblasts in the absence of TBI and on cytokine levels post-TBI at the time of BMT (related to Figure 6) (A) H+E stained metaphyseal bone (BO) bone marrow (BM) sections at low (20x, top) and high (40x, bottom) power in WT mice treated with 7 days of high dose TPO (HDTPO) per the dosing schedule shown in Figure 6A, but in the absence of TBI. Images demonstrates that while TPO does significantly increase numbers of megakaryocytes in BM in the absence of TBI (red arrowheads, top panel), TPO administration alone does not lead to endosteal migration of megakaryocytes or increase osteoblast layers (black arrowheads, bottom panel) above baseline in the absence of TBI. (B) TPO levels in plasma (top) and BM extracts (bottom) from WT mice treated with high dose TPO (HDTPO), low dose TPO (LDTPO) or sham according to the dosing scheme in Figure 6A. Levels were measured on Day 0 of this schedule, the time of BMT in the transplant studies in Figure 6, and 24 hours after the last dose of TPO was given. The data demonstrate no residual increase in TPO levels in the TPO- versus sham-treated groups, demonstrating that the increased engraftment efficiency seen in mice treated with HDTPO versus LDTPO or sham in Figure 6F is not due to increased residual levels of TPO interacting directly with donor HSC post-BMT. (C) PDGF-BB and (D) SDF-1 levels in BM 48 hours post-TBI in mice treated with HDTPO, LDTPO, and sham according to the dosing schedule in Figure 6A, showing that TPO administration did not significantly affect BM levels of either cytokine.